Nuclear Instruments and Methods in Physics Research B 365 (2015) 240–243

Contents lists available at ScienceDirect

Nuclear Instruments and Methods in Physics Research B

journal homepage: www.elsevier.com/locate/nimb

A DLTS study of hydrogen doped czochralski-grown silicon

M. Jelinek [a,*], J.G. Laven [b], S. Kirnstoetter [c], W. Schustereder [a], H.-J. Schulze [b], M. Rommel [d], L. Frey [d,e]

[a] Infineon Technologies Austria AG, 9500 Villach, Austria
[b] Infineon Technologies AG, 81726 Munich, Germany
[c] Institute of Solid State Physics, Graz University of Technology, 8010 Graz, Austria
[d] Fraunhofer Institute of Integrated Systems and Devices IISB, 91058 Erlangen, Germany
[e] Chair of Electron Devices, FAU Erlangen-Nuremberg, 91058 Erlangen, Germany

ARTICLE INFO

Article history:
Received 1 October 2014
Received in revised form 3 June 2015
Accepted 15 July 2015
Available online 28 July 2015

Keywords:
Deep level defects
Proton implantation
Silicon

ABSTRACT

In this study we examine proton implanted and subsequently annealed commercially available CZ wafers with the DLTS method. Depth-resolved spreading resistance measurements are shown, indicating an additional peak in the induced doping profile, not seen in the impurity-lean FZ reference samples. The additional peak lies about 10–15 μm deeper than the main peak near the projected range of the protons. A DLTS characterization in the depth of the additional peak indicates that it is most likely not caused by classical hydrogen-related donors known also from FZ silicon but by an additional donor complex whose formation is assisted by the presence of silicon self-interstitials.

1. Introduction

Proton implantations find wide-spread application in tailoring the electrical characteristics of modern silicon power devices [1]. At moderate activation temperatures below 200 °C proton-induced lattice damage is used to reduce the local minority carrier lifetime, thus improving the switching capability of bipolar devices, such as power thyristors [2]. Another application is the formation of shallow hydrogen-related donors (HDs) at annealing temperatures between 350 °C and 550 °C [3]. The low mass of the protons enables a high penetration depth at acceleration energies that are compatible with commercially available implantation tools. Thus, deep-lying doping profiles beyond a depth of 100 μm are achievable, allowing a well-defined modification of the drift region of vertical power devices. Although the creation of HDs by proton implantation is known since 1970 [4], the microscopic composition of these donor complexes is still under debate. However, various studies on the behavior of hydrogen in silicon [5] and on resistivity changes due to an interaction with electron-induced [6], neutron-induced [7], helium-induced [8], or proton-induced damage [9], lead to an elevated understanding of the present matter. In crystalline silicon, hydrogen can form stable electrically active complexes with vacancy-related defects originating from the initial implant damage. At least part of these complexes act as shallow-level donors with an ionization energy below 56 meV [10,11]. Fig. 1 depicts the two processes necessary for hydrogen-related doping by proton implantation: The initial proton implantation at fluences between, e.g., 10^{13} cm^{-2} and 10^{15} cm^{-2} and a subsequent diffusion of the implanted hydrogen in a temperature regime of 350-500 °C.

The doping efficiency (i.e., the number of HDs generated per implanted proton) of hydrogen doping is influenced by the purity of the substrate material. On the one hand, this is due to the fact that the diffusion of hydrogen is influenced by impurities in the respective silicon substrate (e.g., oxygen) acting as diffusion traps. On the other hand, the overall doping efficiency in CZ substrates is increased compared to FZ substrates by the formation of oxygen-related thermal donors (OTDs) [12], whose formation is additionally enhanced both by the crystal damage induced by the proton implantation (i.e., radiation-enhanced thermal donors, RETDs) [13] and catalytically by the presence of hydrogen itself [14].

Another peculiarity regarding the shape of the donor profiles in proton implanted and annealed CZ grown silicon was shown in Ref. [15], where hydrogen-induced donor profiles were compared for FZ and CZ substrates. The presented data showed that an additional donor peak appears beyond the projected range (R_p) of the protons.[1] More recently, the formation of this additional peak after proton irradiation and subsequent annealing of CZ substrates, in a depth of R_p + (10–15) μm was discussed in Ref. [9]. Depending on the parameters of the annealing step, donor concentrations up to

[1] This effect was not explicitly discussed by the authors of Ref. [15]. However, the authors of the present study recognized the additional donor peak discussed in the following also in the HD-concentration profiles shown in figure 8 of said reference.

* Corresponding author.

http://dx.doi.org/10.1016/j.nimb.2015.07.078
0168-583X/

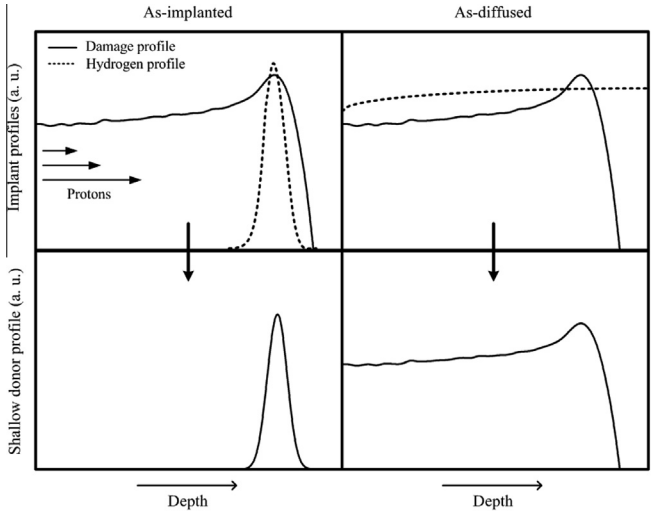

Fig. 1. The hydrogen doping process and related shallow donor profiles. Left: as-implanted – Gaussian shaped donor profile follows the hydrogen distribution. Right: as-diffused – donor profile is in accordance with the distribution of the initial damage.

10% of the main peak's maximum concentration were reported for the additional peak. Thus, the additional peak in CZ silicon has a significant impact on the overall doping efficiency compared to the case in FZ silicon.

The technical application of hydrogen doping is not solely characterized by the generated concentration of shallow-level donors. A characteristic profile of electrically active defects with deep levels (with an ionization energy of more than, e.g., 100 meV) is also formed which affects the carrier lifetime in a device. Thus, a characterization of deep-level defects, e.g., with the DLTS-technique is of importance for a complete understanding of proton-implantation doping. For FZ-substrates there is already a good knowledge about the introduction rates of various deep level defects at different implantation and annealing conditions [9,16]. However, only little is known about defect formation caused by proton implantation in CZ substrates. In particular, the additional donor peak located about 10–15 μm deeper than the main peak was never examined with DLTS before. The reason may be, that the DLTS measurement in an accurately defined depth within a doping profile extending more than, e.g., 10 μm into the depth of the sample is conducted with an elevated experimental effort. It requires either an accurate beveling (as described in, e.g., Ref. [17]) or very high voltages in order to expand the space charge region to the desired measurement depth. The beveling method is not preferred due to the fact that the top metal contact is then inclined with respect to the ohmic backside contact. As a consequence sophisticated modeling of the field line distribution is necessary in order to correctly interpret the DLTS capacitance transients. Similarly, applying high-voltage (>100 V) is not available on most DLTS setups. In addition, the high carrier concentration in the main peak blocks the depletion region from reaching the following additional peak.

Within the present study, we thus applied a mechanical grinding step in order to thin the samples up to the desired region of interest. This approach enabled for the first time a direct characterization of the deep level defects in the additional peak appearing after hydrogen doping in CZ substrates.

2. Experimental

We used commercially available ⟨100⟩-oriented substrate materials grown by the FZ and CZ process respectively. The highly pure FZ wafer was phosphorus doped with a resistivity of 120 Ω cm. Fourier-transform infrared spectroscopy (FTIR) measurements (the used setup is specified in Ref. [18]) indicated that the oxygen concentration [O_i] was below 1×10^{16} cm^{-3}. The CZ wafers had a resistivity of 6 kΩ cm and an oxygen concentration [O_i] of 2×10^{17} cm^{-3}. In order to reduce possible point defect agglomerates originating from the crystal growth process, all wafers were exposed to an oxidizing high-temperature step at 1100 °C prior to any further processing. The wafers were implanted with 4 MeV protons at an angle of 7° relative to the normal of the wafer surface with a fluence of 1.7×10^{14} cm^{-2} and subsequently annealed for 5 h at a temperature of 470 °C under nitrogen atmosphere. The projected range of the 4-MeV protons was in a depth of 148 μm. Shallow HD profiles were recorded by spreading resistance profiling (SRP) measurements [19] with a beveling angle of 11.5° yielding a depth resolution of 0.9 μm. For DLTS measurements the CZ wafers were thinned from the front side (meaning the irradiated side of the wafer) up to a depth of 70 μm (sample A) or 150 μm (sample B) subsequent to implantation and furnace annealing. The thinning process consisted of a mechanical grinding step followed by a dry polish. With this method two different regions of the respective hydrogen donor profiles were examined according to Fig. 2. Schottky contacts were realized by Au-evaporation and the ohmic backside contact was established by rubbing in a GaIn-eutectic. Majority carrier Fourier-transform DLTS measurements were performed on a PhysTech HERA-DLTS system using a time window of 20.48 ms. The bias and filling pulse voltage was −1.0 V and −0.3 V respectively with a pulse length of 1 ms.

3. Results and discussion

Fig. 3 depicts SRP results showing the shallow HD profiles generated by the specified hydrogen doping process for two different substrates. In both substrates a main HD peak appears coinciding with the end-of-range implant damage peak, whose position matches well with SRIM [20] simulation. However, the additional peak appearing in the CZ substrate cannot be explained by the simulation. The distance between the main peak and the additional peak is independent on the implant energy [9]. Regarding the width of the additional peak, a dose dependency was reported though. This lead to the assumption, that the donor complex responsible for the formation of the additional peak is related to the diffusion of silicon self-interstitials Si_i. Si_i was suggested to enhance the formation of a carbon related donor complex by the substitution reaction [21]:

$$C_s + Si_i \rightarrow C_i \quad (1)$$

The additional peak was also detected directly after proton implantation, without an additional annealing step [22], further supporting the participation of Si_i, which is known to be mobile at room temperature [23]. With this assumption it becomes obvious that in Fig. 3, the additional peak does not appear in the profiles of the FZ substrate due to its lower carbon content.

Fig. 4 shows DLTS spectra indicating the appearing defects within the damaged region (thinned sample A) and the additional peak (thinned sample B) region of the CZ profile shown in Fig. 3. In total 8 deep levels were detected within this study denoted as traps A–H. The measured energy levels and cross sections are listed in Table 1 together with their preliminary assignment to known defects according to the references given. A more detailed discussion on the assignment of defects found after proton implantation and subsequent annealing is given in Ref. [16]. It appears that the vacancy-related traps E–H are solely present in sample A, indicating a crucial difference in the (local) defect chemistry between the

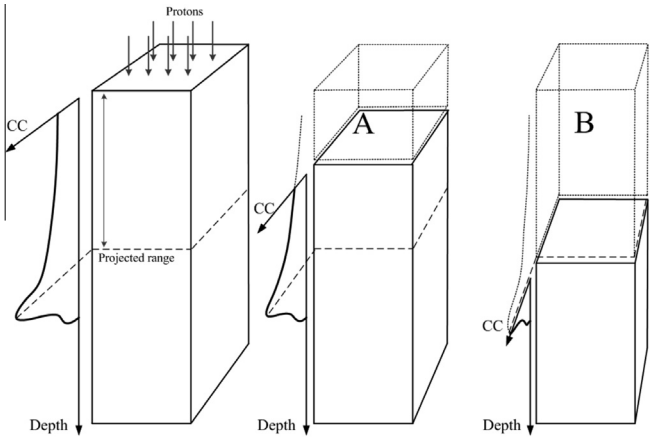

Fig. 2. DLTS sample preparation of the samples A and B according to the two thinning processes indicated.

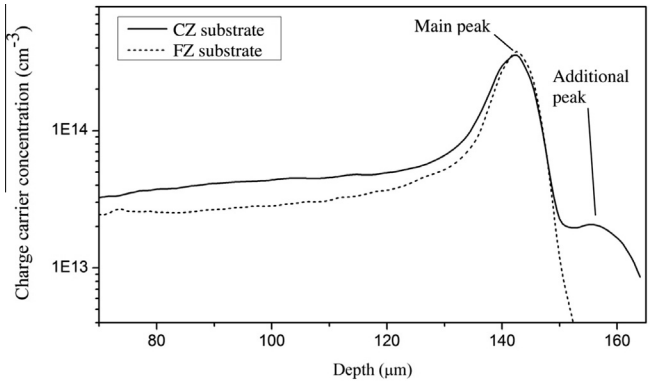

Fig. 3. Comparison of donor profiles in proton implanted FZ- and CZ silicon. The proton fluence was 1.7×10^{14} at an energy of 4 MeV. Both samples were annealed 5 h under nitrogen atmosphere at a temperature of 470 °C. The charge carrier profiles are substracted by the substrate doping concentration.

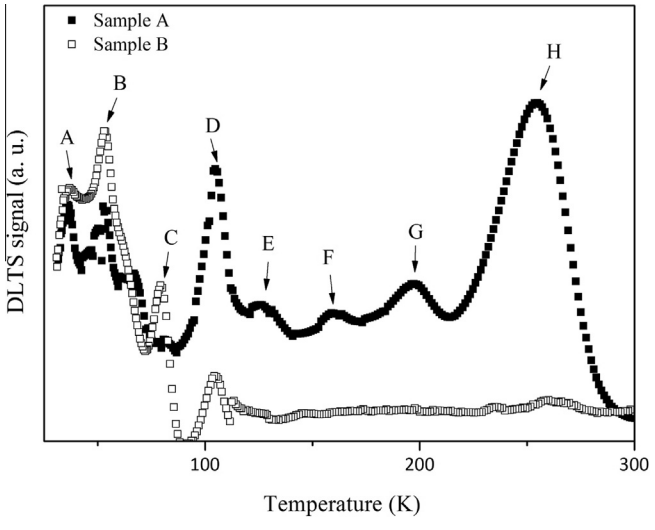

Fig. 4. DLTS spectra of proton implanted and annealed samples in the damaged region of the profile (sample A) and in the additional peak (sample B). The spectra are normalized to the spectrum of sample A.

two depths evaluated in the respective samples. This fact becomes reasonable if the local conditions at the respective depths within the implantation damage profiles are considered. Sample B was thinned beyond the main damage peak around the projected range.

Table 1
Deep levels detected in the samples A (1) and B (2).

Trap	$E_C - E_T$ (meV)	σ (10^{-15} cm^{-2})	Preliminary assignment	Related references
$A^{1,2}$	69	4	$OTDD^{0/+a}$	[26]
$B^{1,2}$	108	186	C_iO_i–$H^{-/0}$	[27]
$C^{1,2}$	147	5	$OTDD^{+/2+}$	[28]
$D^{1,2}$	204	17	Unknown	–
E^1	213	48	$(V_2O^{2-/-})$	[29]
F^1	343	73	Unknown $VOH^{-/0}$?	[30]
G^1	418	39	$V_2O_2^{-/0}$	[31]
H^1	433	45	$V_2H^{-/0} + V_2^{-/0}$	[9]

[a] Oxygen-related thermal double donor.

Directly after implantation the main part of the introduced initial implant damage (i.e., Frenkel pairs) in this region vanishes rapidly due to recombination [24]. Remaining vacancy-related complexes are present in form of monovacancies (V), divacancies (V_2), or higher order complexes such as the very stable and electrically inactive V_6 complex [25]. Due to the low mobility of V_2 and higher order vacancy complexes it is not expected to see any V-related deep levels beyond the end of range damage region. However, the mobile self-interstitials can diffuse beyond the projected range. There they find no recombination partners and can therefore contribute to the substitution reaction (1), which in turn promotes the donor complex formation in the additional peak region. It is to be noted that the traps A–D are also found in the damaged region of the doping profile, in accordance with Ref. [9]. However, the local defect chemistry within the additional peak, for the first time indirectly confirms previous assignments [9,16,27] of carbon contributing to the trap E_C – 108 meV.

4. Conclusion

For proton implanted and annealed samples, an additional donor peak beyond the main hydrogen-related donor peak was observed in CZ-grown material. The additional peak does not appear in FZ-grown substrate. An involvement of impurities originating from the crystal growth process, such as carbon, thus seems likely. DLTS results indicate that no vacancy-related deep levels are formed in the region of this additional peak. Thus there is evidence that the donors in the additional peak do not consist of classical hydrogen-related donors, which are assumed to be hydrogen-decorated vacancy complexes. In fact, it was shown that the detected deep level traps in the additional peak match with an explanation implying fast diffusing self-interstitials that substitute carbon on a lattice site, which in turn contributes to related defect formation.

References

[1] R. Job, J.G. Laven, F.-J. Niedernostheide, H.-J. Schulze, H. Schulze, W. Schustereder, Phys. Status Solidi B 209 (2012) 10.
[2] D.C. Sawko, J. Bartko, I.N. Sneddon, IEEE Trans. Nucl. Sci. 30 (1983) 2.
[3] W. Wondrak, Erzeugung von Strahlenschäden in Silizium durch hochenergetische Elektronen und Protonen (Ph.D. thesis), Johann-Wolfgang-Goethe-Universität, 1985.
[4] G.H. Schwuttke, K. Brack, E.F. Gorey, A. Kahan, L.F. Lowe, Rad. Eff. 6 (1970) 1.
[5] O.S. Andersen, Electrical Properties of Hydrogen-related Defects in Crystalline Silicon (Ph.D. thesis), University of Manchester, 2002.
[6] V.P. Markevich, M. Suezawa, K. Sumino, L.I. Murin, J. Appl. Phys. 76 (1994) 11.
[7] J. Hartung, J. Weber, L. Genzel, Mater. Sci. Forum 65–66 (1990).
[8] R. Job, F.-J. Niedernostheide, H.-J. Schulze, H. Schulze, Mater. Res. Soc. Symp. Proc. 1195 (2010) 2.
[9] J.G. Laven, Protonendotierung von Silizium, Springer Vieweg, 2014.
[10] J. Hartung, J. Weber, Mater. Sci. Eng., B 4 (1989) 1–4.
[11] J. Hartung, J. Weber, Phys. Rev. B 48 (1993) 19.
[12] W. Kaiser, H.L. Frisch, H. Reiss, Phys. Rev. 112 (1958) 5.
[13] R. Pflueger, J.C. Corelli, J.W. Corbett, Phys. Status Solidi A 91 (1985) 1.

[14] H.J. Stein, S. Hahn, J. Electrochem. Soc. 142 (1995) 4.
[15] V. Komarnitskyy, P. Hazdra, ECS Trans. 25 (2009) 3.
[16] J.G. Laven, M. Jelinek, R. Job, W. Schustereder, H.-J. Schulze, M. Rommel, L. Frey, Phys. Status Solidi B 251 (2014) 11.
[17] E. Badr, P. Pichler, G. Schmidt, J. Appl. Phys. 116 (2014) 13.
[18] H.Ch. Alt, Y. Gomeniuk, B. Wiedemann, H. Riemann, J. Electrochem. Soc. 150 (2003) 8.
[19] R.G. Mazur, D.H. Dickey, J. Electrochem. Soc. 113 (1966) 3.
[20] Z.F. Ziegler, M.D. Ziegler, J.P. Biersack, Nucl. Instr. Phys. Res. B 268 (2010) 11–12.
[21] G.D. Watkins, K.L. Brower, Phys. Rev. Lett. 36 (1976) 22.
[22] S. Kirnstoetter, M. Faccinelli, P. Hadley, M. Jelinek, W. Schustereder, J.G. Laven, H.-J. Schulze, 2014 IIT Conference.
[23] P. Pichler, Intrinsic Point Defects, Impurities, and Their Diffusion in Silicon, Springer, 2004.
[24] H. Ryssel, I. Ruge, Ionenimplantation, Vieweg+Teubner Verlag, 1978.
[25] S.K. Estreicher, J.L. Hastings, P.A. Fedders, Appl. Phys. Lett. 70 (1997) 4.
[26] L.C. Kimerling, J.L. Benton, Appl. Phys. Lett. 39 (1981) 5.
[27] V.P. Markevich, I.F. Medvedeva, L.I. Murin, T. Sekiguchi, M. Suezawa, K. Sumino, Mater. Sci. Forum 196–201 (1995).
[28] E. Simoen, C. Claeys, J.M. Rafi, A.G. Ulyashin, Mater. Sci. Eng., B 134 (2006) 2–3.
[29] P. Pellegrino, P. Leveque, J. Lalita, A. Hallen, C. Jagadish, B.G. Svensson, Phys. Rev. B 64 (2001) 19.
[30] K. Irmscher, H. Klose, K. Maass, J. Phys. C 17 (1984) 35.
[31] J. Coutinho, R. Jones, S. Öberg, P.R. Briddon, Physika B 340–342 (2003).